Dai *et al. Molecular Cancer* (2025) 24:79
https://doi.org/10.1186/s12943-025-02285-y

Molecular Cancer

RESEARCH Open Access

NNMT promotes acquired EGFR-TKI resistance by forming EGR1 and lactate-mediated double positive feedback loops in non-small cell lung cancer

Jiali Dai[1†], Xiyi Lu[1†], Chang Zhang[2†], Tianyu Qu[1†], Wei Li[1], Jun Su[3], Renhua Guo[1], Dandan Yin[4*], Pingping Wu[5*], Liang Han[6*] and Erbao Zhang[2,7*]

Abstract

Background Epidermal growth factor receptor-tyrosine kinase inhibitors (EGFR-TKIs) are remarkably effective for treating EGFR-mutant non-small cell lung cancer (NSCLC). However, patients inevitably develop acquired drug resistance, resulting in recurrence or metastasis. It is important to identify novel effective therapeutic targets to reverse acquired TKI resistance.

Results Bioinformatics analysis revealed that nicotinamide N-methyltransferase (NNMT) was upregulated in EGFR-TKI resistant cells and tissues via EGR1-mediated transcriptional activation. High NNMT levels were correlated with poor prognosis in EGFR-mutated NSCLC patients, which could promote resistance to EGFR-TKIs in vitro and in vivo. Mechanistically, NNMT catalyzed the conversion of nicotinamide to 1-methyl nicotinamide by depleting S-adenosyl methionine (the methyl group donor), leading to a reduction in H3K9 trimethylation (H3K9me3) and H3K27 trimethylation (H3K27me3) and subsequent epigenetic activation of EGR1 and ALDH3A1. In addition, ALDH3A1 activation increased lactic acid levels, which further promoted NNMT expression via p300-mediated histone H3K18 lactylation on its promoter. Thus, NNMT mediates the formation of a double positive feedback loop via EGR1 and lactate, EGR1/NNMT/EGR1 and NNMT/ALDH3A1/lactate/NNMT. Moreover, the combination of a small-molecule inhibitor for NNMT (NNMTi) and osimertinib exhibited promising potential for the treatment of TKI resistance in an NSCLC osimertinib-resistant xenograft model.

†Jiali Dai, Xiyi Lu, Chang Zhang and Tianyu Qu contributed equally to this work and should be regarded as joint first authors.

*Correspondence:
Dandan Yin
jsnydandan@sina.com
Pingping Wu
pingpingwu_njmu@163.com
Liang Han
hanliang_njmu@sina.com
Erbao Zhang
erbaozhang@njmu.edu.cn

Full list of author information is available at the end of the article

Conclusions The combined contribution of these two positive feedback loops promotes EGFR-TKI resistance in NSCLC. Our findings provide new insight into the role of histone methylation and histone lactylation in TKI resistance. The pivotal NNMT-mediated positive feedback loop may serve as a powerful therapeutic target for overcoming EGFR-TKI resistance in NSCLC.

Keywords EGFR-TKI resistance, Histone methylation, Histone lactylation, Lung cancer

Background

Lung cancer is the leading cause of cancer-related mortality worldwide [1]. Approximately 85% of lung cancers are non-small cell lung cancer (NSCLC) [2]. EGFR tyrosine kinase inhibitors (EGFR-TKIs) reportedly improve outcomes in patients with advanced EGFR-mutant NSCLC [3–6]. However, despite the initial remarkable response, patients inevitably develop acquired drug resistance to EGFR-TKI treatment, leading to recurrence or metastasis. The underlying molecular mechanisms of EGFR-TKI resistance are not fully understood. Thus, there is an urgent need to elucidate this new mechanism and identify novel effective therapeutic targets to reverse acquired TKI resistance.

Epigenetic modifications, including DNA methylation, histone modification and RNA modification, play key roles in cancer progression [7–9]. Moreover, many studies have shown that epigenetic modifications are highly important in regulating tumor drug resistance [10–12]. For example, METTL3-mediated RNA methylation promotes tumor development and chemotherapy resistance [13]. Our previous studies revealed that histone methylation and RNA modifications can regulate gene expression and participate in tumorigenesis and drug resistance [14–18]. In terms of epigenetic regulation, histone modifications regulate DNA accessibility, chromatin structure and dynamics, and gene expression. These modifications regulate chromatin relaxation and gene transcription or chromatin condensation and gene repression, respectively [19]. The dysregulation of histone modifications can shift the balance between transcription activation and inhibition, leading to the occurrence and development of disease as well as tumor resistance [20]. Histones can be modified via acetylation, methylation, phosphorylation, ubiquitination, etc [19]. More recently, lactate-derived histone lactylation was identified as an epigenetic modification that activates gene transcription. Lactylation of lysine residues of histones (Kla) was first described in 2019 [21]. However, the role of histone lactylation in TKI resistance remains unclear.

NNMT is an epigenetic modification enzyme that catalyzes the transfer of the methyl group from S-adenosyl-l-methionine (SAM) to nicotinamide to generate S-adenosylhomocysteine (SAH) and 1-methylnicotinamide (1-MNA). Therefore, NNMT could regulate the epigenetic state of histone methylation in target genes. Accumulating evidence has demonstrated that NNMT is overexpressed in various tumors and is associated with tumorigenesis and chemotherapy resistance [22, 23]. However, little is known about the role of NNMT in TKI resistance in lung cancer. In addition, the communication between histone methylation and histone lactylation has yet to be defined.

In this study, we aimed to elucidate the novel mechanism by which NNMT regulates EGFR-TKI resistance in NSCLC. We found that NNMT guides histone epigenetic modifications and activates EGR1 and ALDH3A1 in the context of EGFR-TKI resistance. ALDH3A1 also increases lactic acid levels. NNMT mediates two positive feedback regulatory loops, EGR1/NNMT/EGR1 and NNMT/ALDH3A1/lactate/NNMT, which coordinately promote EGFR-TKI resistance. Our findings provide new insight into the role of histone methylation and histone lactylation in TKI resistance. The pivotal NNMT-mediated regulatory loop represents a potential target for overcoming EGFR-TKI resistance in lung cancer.

Methods

Data retrieval and analysis

Microarray datasets were accessed from the Gene Expression Omnibus (GEO) database (https://www.ncbi.nlm.nih.gov/geo/) using the R package "GEOquery". Four microarray datasets, namely, GSE193258, GSE114647 and GSE123066, were obtained. GSE193258 contained osimertinib-sensitive H1975 cells ($n = 3$), osimertinib-resistant H1975 cells ($n = 6$), osimertinib-sensitive PC9 cells ($n = 3$), and osimertinib-resistant PC9 cells ($n = 6$). GSE114647 contained osimertinib-sensitive H1975 cells ($n = 3$) and osimertinib-resistant H1975 cells ($n = 3$). GSE123066 included gefitinib-sensitive HCC4006 cells ($n = 3$) and gefitinib-resistant HCC4006 cells ($n = 3$). The differentially expressed genes (DEGs) were analyzed using the R package "limma" with a false discovery rate (FDR) of $q < 0.05$ and a fold change ≥ 1.5.

Tissue collection and ethics statement

Patients harboring an EGFR exon 19 deletion (Exon 19 Del) or a point mutation in exon 21 (Exon 21 L858R) were included in this study. All patients in this category had histopathologically diagnosed primary lung cancer and previously received first-line treatment with an EGFR-TKI. Regular imaging examinations were performed regularly, usually every 6–8 weeks, to evaluate the changes in tumors according to the Response Evaluation Criteria

in Solid Tumors version 1.1 (RECIST1.1) standard [24], and progressive disease (PD) was defined as EGFR-TKI resistance. The study was approved by the Ethics Committee on Human Research of the First Affiliated Hospital of Nanjing Medical University and was performed in compliance with the Helsinki Declaration. The written informed consent was obtained from all patients.

Cell culture

PC9 and HCC827 cell lines were purchased from the cell library of the Chinese Academy of Sciences (Shanghai, China). Gefitinib-resistant cells (PC9/GR and HCC827/GR) and osimertinib-resistant cells (PC9/OR and HCC827/OR) were generated as described previously [25]. Briefly, the corresponding parental PC9 and HCC827 cells were exposed to concentrations of gefitinib starting at 50 nM (osimertinib starting at 10 nM) until they could proliferate freely in the presence of a certain concentration of gefitinib or osimertinib, which occurred after 25 weeks of TKI drug treatment. PC9, PC9/GR, and PC9/OR cells were cultured in DMEM, and HCC827, HCC827/GR, and HCC827/OR cells were cultured in RPMI 1640 medium. All media were supplemented with 10% fetal bovine serum and 1% penicillin–streptomycin. All the cells were incubated at 37 ℃ and 5% CO2.

Cell transfection

Specific siRNA and negative control siRNA (si-NC) transfection was performed using Lipofectamine 2000 Transfection Reagent (Invitrogen, USA). The sequences of the siRNAs are listed in Table S3. The plasmids were transfected into lung cells using X-tremeGENE™ HP DNA Transfection Reagent (Roche, USA) according to the manufacturer's protocol. After 48 h of transfection, the cells were harvested for subsequent experiments.

RNA extraction and qRT–PCR analyses

The cells were collected, and total RNA was extracted with TRIzol reagent (Invitrogen, USA). The RNA was reverse transcribed into cDNA using a reverse transcription kit (Takara). RT–qPCR was subsequently performed using a TB Green RT–qPCR kit according to the manufacturer's instructions. β-Actin was used as the reference gene, and all the primers used are listed in Table S3. All the experiments were repeated three times.

Cell proliferation assay

Cell viability was determined using an MTT assay kit (Sigma, USA) according to the manufacturer's instructions. For the colony formation assay, a certain number of cells were plated into a six-well plate and maintained in culture media supplemented with 10% FBS for 2 weeks. At the same time, the medium was changed every four days. After approximately 2 weeks, the clones were fixed with methanol, stained with 0.1% crystal violet and photographed. Colonies were counted to evaluate the clonogenic capabilities of the cells. The EdU assay was performed with an EdU assay kit (RiboBio, China) according to the manufacturer's instructions. All the experiments were repeated three times.

Flow cytometric analysis

After 48 h of transfection, the cells were harvested and stained with fluorescein isothiocyanate (FITC)-annexin V and propidium iodide according to the manufacturer's instructions for the FITC Annexin V programmed cell death detection kit (BD Biosciences). Flow cytometry was used to detect apoptotic cells. Cell viability was quantified by counting the number of viable, dead, early apoptotic, and late apoptotic cells. The proportion of apoptotic cells was calculated on the basis of the number of early apoptotic cells and late apoptotic cells. All the experiments were repeated three times.

Dual-luciferase reporter assay

The cells were cotransfected with the luciferase vector and Renilla luciferase plasmid. After 48 h of transfection, dual-luciferase reporter assays were conducted via the Dual-Luciferase® Reporter Assay System Kit (Promega) according to the manufacturer's instructions. The firefly luciferase luminescence data were normalized to the Renilla luciferase luminescence data. All the experiments were repeated three times.

Chromatin immunoprecipitation (ChIP) assay

ChIP experiments were performed using an EZ-CHIP Kit (Millipore) according to the manufacturer's protocol. The specific antibodies for histone H3 monomethylated at Lys27 (H3K27me3, Cat. # A22006) and histone H3 monomethylated at Lys9 (H3K9me3, Cat. # A22295) were purchased from ABclonal. The specific antibody for H3K18la was purchased from PTM. The specific antibody for EGR1 (Cat. # 4154) was purchased from Cell Signaling Technology. The ChIP primer sequences are listed in Table S3. The immunoprecipitated DNA was quantified via qRT–PCR. The ChIP data are expressed as percentages of input DNA according to the following equation: $2^{[\text{Input Ct}-\text{Target Ct}]}\times 100$ (%). All the experiments were repeated three times.

ALDEFLUOR flow cytometry assay

The ALDEFLUOR assay was performed using the ALDEFLUOR Kit (Stem Cell Technologies, Vancouver, BC, Canada) according to the manufacturer's protocol. The corresponding cells were suspended in 500 μL ALDEFLUOR assay buffer containing the ALDH substrate and then incubated at 37 °C for 30 min. The cell samples were examined using a FACSCalibur flow cytometer (BD

Biosciences, San Jose, CA, USA), and the data were analyzed using FlowJo software (BD Biosciences). All the experiments were repeated three times.

SAM and SAH concentrations

The concentrations of intracellular SAM and SAH were measured using the SAM and SAH ELISA kits (Cell Biolabs, USA) according to the manufacturer's instructions. The SAM/SAH ratios were measured and compared. All the data were normalized to the total amount of protein. All the experiments were repeated three times.

ATP and lactate concentrations

The ATP concentration in the cells was determined using the ATP Determination Kit (Beyotime, China) according to the manufacturer's instructions. The lactate concentration was determined using a Lactate Assay Kit (Sigma). All the data were normalized to the number of cells. All the experiments were repeated three times.

ECAR assay

ECAR was determined using a Seahorse XF96 flux analyzer (Seahorse Bioscience, USA). The cells were stimulated with Glu, oligomycin and 2-DG to measure the changes in ECAR. All the experiments were repeated three times.

Western blot analysis and antibodies

Total proteins from the cells were harvested using RIPA buffer (Beyotime, China) and separated using SDS–PAGE. Proteins were then transferred to PVDF membranes (Millipore) using standard protocols and incubated with specific antibodies. Finally, the membrane was visualized by an imaging system (Bio-Rad, USA). An anti-β-Actin antibody was used as a control. The anti-NNMT antibody (dilution ratio, 1:1000; Cat. # ab119758) was purchased from Abcam. Anti-EGR1 (dilution ratio, 1:1000; Cat. # 4154) and anti-p300 (dilution ratio, 1:1000; Cat. #54062) antibodies were purchased from Cell Signaling Technology. Anti-β-Actin (dilution ratio, 1:10000, Cat. # 66009-1-Ig), anti-H3 (dilution ratio, 1:1000, Cat. # 17168-1-AP), and anti-ALDH3A1 (dilution ratio, 1:1000, Cat. # 15578-1-AP) antibodies were purchased from Proteintech. Anti-H3K27me3 (dilution ratio, 1:1000, Cat. # A22006) and anti-H3K9me3 (dilution ratio, 1:1000, Cat. # A22295) antibodies were purchased from ABclonal. Anti-pan-Kla (dilution ratio, 1:1000, Cat. # PTM-1401RM) and anti-H3K18la (dilution ratio, 1:1000, Cat. # PTM-1406RM) antibodies were purchased from PTM. All the experiments were repeated three times. All uncropped blots are presented in the supplemental data files.

Animal xenograft tumor model

Five-week-old male BALB/c nude mice were purchased from the Animal Center of the Chinese Academy of Science (Shanghai, China). The mice were housed under specific pathogen-free (SPF) and controlled conditions (24–26 °C, 40–70% humidity) with a 12-hour light/dark cycle. To establish xenograft models, stably transfected PC9/OR cells (5×10^6 cells in 100 μl of PBS) were injected subcutaneously into nude mice. After the tumor volume reached the appropriate size, the mice were randomly divided into control and treatment groups so that each group had an equivalent distribution of initial tumor sizes following the administration of osimertinib or NNMTi (MedChemExpress, MCE). The mice were administered osimertinib (25 mg/kg/day) orally, NNMTi (10 mg/kg/day) intraperitoneally, osimertinib plus NNMTi or vehicle control. The tumor volumes were measured daily. The tumor volume was calculated as $0.5 \times \text{length} \times \text{width}^2$. At the end of the experiment, the nude mice were euthanized, and the tumor tissues were removed and weighed. Tumor samples were subjected to hematoxylin and eosin (HE) staining and immunohistochemistry (IHC) analysis. All the animal experiments were conducted with the approval of the Committee on the Ethics of Animal Experiments of Nanjing Medical University and in accordance with the Guide for the Care and Use of Laboratory Animals of the National Institutes of Health.

Statistical analysis

Data analysis was performed using SPSS (IBM, SPSS, USA) and GraphPad Prism software (GraphPad Software, USA). Student's t test, the X^2 test, or the Wilcoxon test were used to compare the variables. Two-sided p values of 0.05 were considered statistically significant.

Results

Bioinformatics analyses of RNA expression profiling data reveal the role of NNMT in EGFR-TKI resistance in lung cancer

To explore the potential genes that may be involved in TKI resistance, we searched for aberrantly expressed genes in the GEO databases (GSE193258, GSE114647, and GSE123066). As shown in Fig. 1A, the expression of several genes was elevated (fold change ≥ 1.5) in TKI-resistant cells compared with TKI-sensitive cells. Nicotinamide N-methyltransferase (NNMT) and calponin 1 (CNN1) were both upregulated in all four datasets. To further validate the relationship between NNMT and EGFR-TKI resistance, we collected 40 tissue samples from patients with advanced NSCLC harboring an EGFR exon 19 deletion (Exon 19 Del) or a point mutation in exon 21 (Exon 21 L858R) (Table S1). All 40 patients had received EGFR-TKI therapy as a first-line treatment. qRT–PCR analysis was conducted to determine NNMT

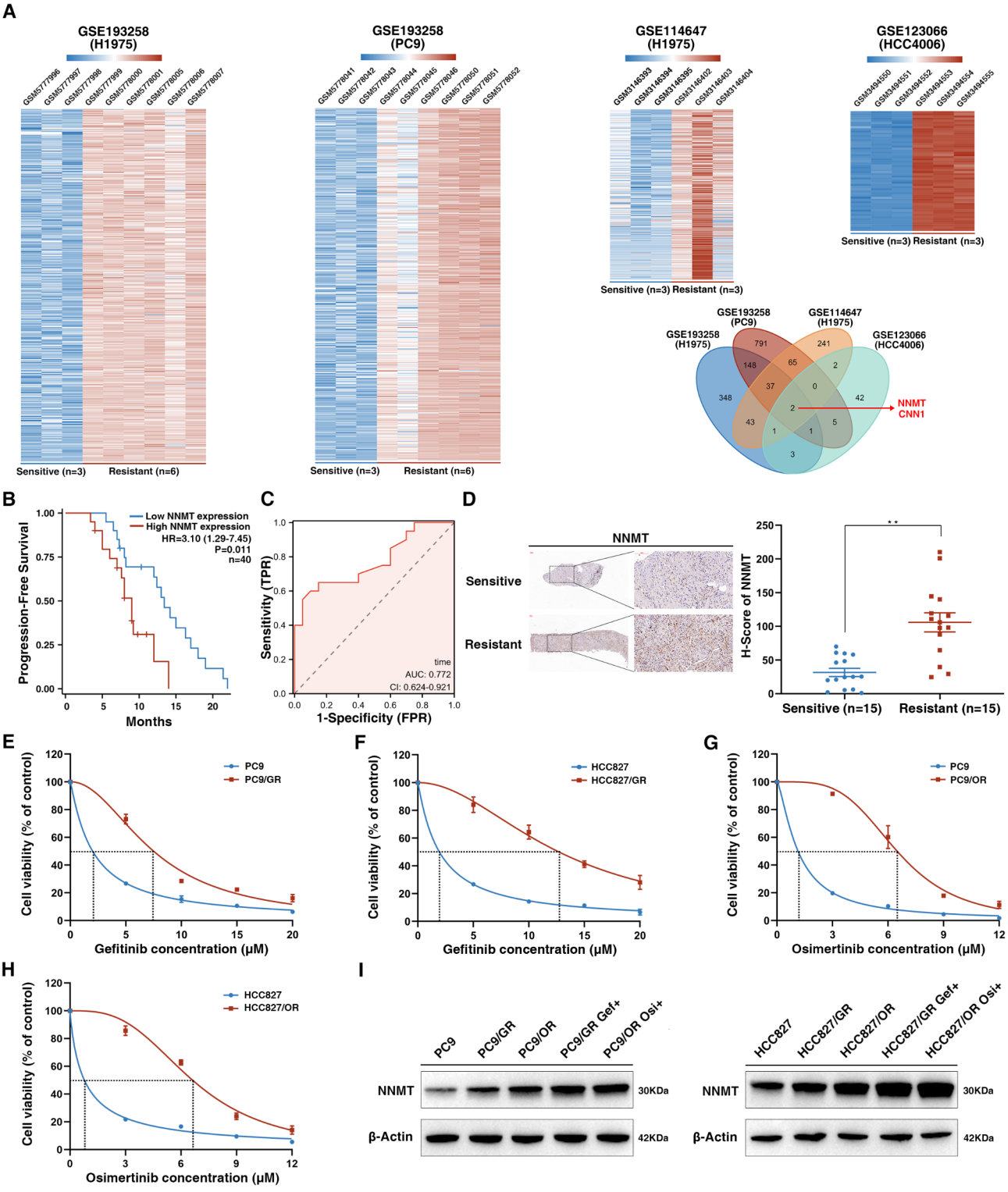

Fig. 1 Bioinformatics analyses of RNA expression profiling data reveal the role of NNMT in EGFR-TKI resistance in lung cancer. (**A**) Activated genes in TKI-resistant cells in these GEO datasets (GSE193258, GSE114647, and GSE123066). (**B**) Higher NNMT expression is associated with a poorer prognosis in patients.(**C**) The ROC curve suggests that NNMT expression serves as a predictive marker for EGFR-TKI resistance. (**D**) NNMT was expressed at higher levels in tissues from TKI-resistant patients than in tissues from TKI-sensitive patients. (**E**, **F**) IC50 values of gefitinib in gefitinib-resistant cells (PC9/GR, HCC827/GR) and their respective parental cells (PC9, HCC827) were examined using the MTT assay. (**G**, **H**) The IC50 values of osimertinib in osimertinib-resistant cells (PC9/OR, HCC827/OR) and their respective parental cells (PC9, HCC827) were examined using the MTT assay. (**I**) Treatment with EGFR-TKIs (gefitinib or osimertinib) increased NNMT expression in TKI-resistant cell lines. Three independent experiments were performed. $^{**}P < 0.01$

and CNN1 expression in tissues from the 40 patients. The 40 patients were subsequently divided into a high group and a low group on the basis of the median expression value of NNMT or CNN1. Among patients treated with EGFR-TKIs, high NNMT expression was associated with a poorer prognosis (Fig. 1B), whereas CNN1 expression had no impact on the prognosis of patients (Figure S1A). Therefore, we focused on the NNMT. Moreover, the ROC curve suggested that NNMT expression levels predict the risk of EGFR-TKI resistance in lung cancer (Fig. 1C). We also collected 15 paired tissue samples from patients before (the sensitive group) and after developing resistance to TKI (the resistant group) (Table S2). Among these patients, 6 received gefitinib, and 9 received osimertinib as the first-line treatment. Immunohistochemical analysis revealed that the TKI-resistant group presented increased NNMT expression compared with the sensitive group (Fig. 1D).

We then constructed PC9 and HCC827 TKI-resistant cell lines, including gefitinib-resistant cell lines (PC9/GR and HCC827/GR) and osimertinib-resistant cell lines (PC9/OR and HCC827/OR) (Fig. 1E - H) (detailed information is included in the methods section). As shown in Fig. 1I, compared with TKI-sensitive cell lines, TKI-resistant cell lines treated with EGFR-TKIs presented increased NNMT expression.

NNMT regulates EGFR-TKI resistance in NSCLC cells

To further explore the biological characteristics of NNMT in EGFR-TKI resistant cells, small interfering RNA (siRNA)-mediated knockdown and plasmid-mediated overexpression were used to manipulate NNMT expression (Figure S1B-S1D). MTT assays revealed that NNMT knockdown significantly decreased the 50% inhibitory concentration (IC50) in TKI-resistant cells (Fig. 2A, Figure S1E), whereas NNMT overexpression significantly increased resistance to EGFR-TKIs in PC9 and HCC827 cells (Fig. 2A, Figure S1E). The MTT assay results also revealed that NNMT knockdown reduced resistance to EGFR-TKIs and cell proliferation in TKI-resistant cells (Fig. 2B, Figure S1F), whereas NNMT overexpression in sensitive cells increased cell proliferation (Fig. 2B, Figure S1F). Compared with that of the control cells, the colony formation capacity of the NNMT-knockdown cells was significantly lower (Fig. 2C, Figure S1G). Regardless of EGFR-TKI treatment, NNMT overexpression increased the capacity for colony formation (Fig. 2C, Figure S1G). Furthermore, the EdU assay results demonstrated that the percentage of EdU-positive cells was lower in the NNMT-knockdown group than in the NNMT-overexpressing group (Fig. 2D). Moreover, NNMT knockdown significantly increased apoptosis in TKI-resistant cells compared with control cells (Fig. 2E).

Direct transcriptional activation of EGR1 contributes to the high NNMT expression in TKI resistance

To gain insight into the mechanism underlying the transcriptional regulation of NNMT, we searched for a transcription factor in the NNMT promoter and identified a potential conserved binding site, early growth response 1 (EGR1), in the NNMT promoter region (Fig. 3A). Previous studies have reported that EGR1 plays a vital role in tumorigenesis and drug resistance [26–28]. We found that EGR1 significantly promotes resistance to EGFR-TKIs and cell proliferation using MTT and colony formation assays (Figure S2A-S2C). Our Western blot analysis revealed that EGR1 knockdown in TKI-resistant cells (PC9/OR, HCC827/OR and HCC827/GR cells) decreased NNMT expression, whereas EGR1 overexpression upregulated NNMT expression (Fig. 3B and Figure S2D). A dual-luciferase reporter assay revealed that deletion of the EGR1 binding site in the NNMT promoter significantly decreased luciferase activity compared with the full-length promoter in PC9/OR, HCC827/OR and HCC827/GR cells (Fig. 3C and Figure S2E). Cotransfection of wild-type binding sites of EGR1 and si-EGR1 in PC9/OR, HCC827/OR and HCC827/GR cells significantly decreased luciferase activity, but cotransfection of mutant binding sites of EGR1 and si-EGR1 had no effect on luciferase activity (Fig. 3D and Figure S2F). Moreover, EGR1 overexpression increased the luciferase activity of the wild-type promoter of EGR1 but had no effect on the mutant type (Fig. 3E and Figure S2F). A ChIP assay also confirmed that EGR1 could directly bind to the NNMT promoter region. EGR1 knockdown reduced the binding enrichment in the NNMT promoter region, whereas EGR1 overexpression increased the enrichment (Fig. 3F and Figure S2G-S2H). In addition, NNMT knockdown partially reversed the effect of EGR1-mediated resistance to TKIs and promoted the proliferation of NSCLC cells, including PC9/OR, HCC827/OR and HCC827/GR cells (Fig. 3G - I and Figure S2I-S2K).

NNMT reduces H3K9me3 and H3K27me3, leading to epigenetic activation of EGR1 and ALDH3A1 and promoting the resistance of NSCLC to EGFR-TKIs

To further analyze the mechanism by which NNMT regulates TKI resistance, RNA sequencing was performed to identify potential targets that might be regulated by NNMT (Fig. 4A and B and Table S4). GO analysis revealed enrichment of metabolic processes, cell proliferation and cell apoptosis (Fig. 4C). Some of these representative genes were verified using qRT–PCR analysis (Fig. 4D). Specifically, NNMT knockdown downregulated the gene expression of EGR1 and aldehyde dehydrogenase 3A1 (ALDH3A1), which are closely related to cell proliferation and metabolism (Fig. 4D). We next conducted Western blot assays and found that

Figure 2

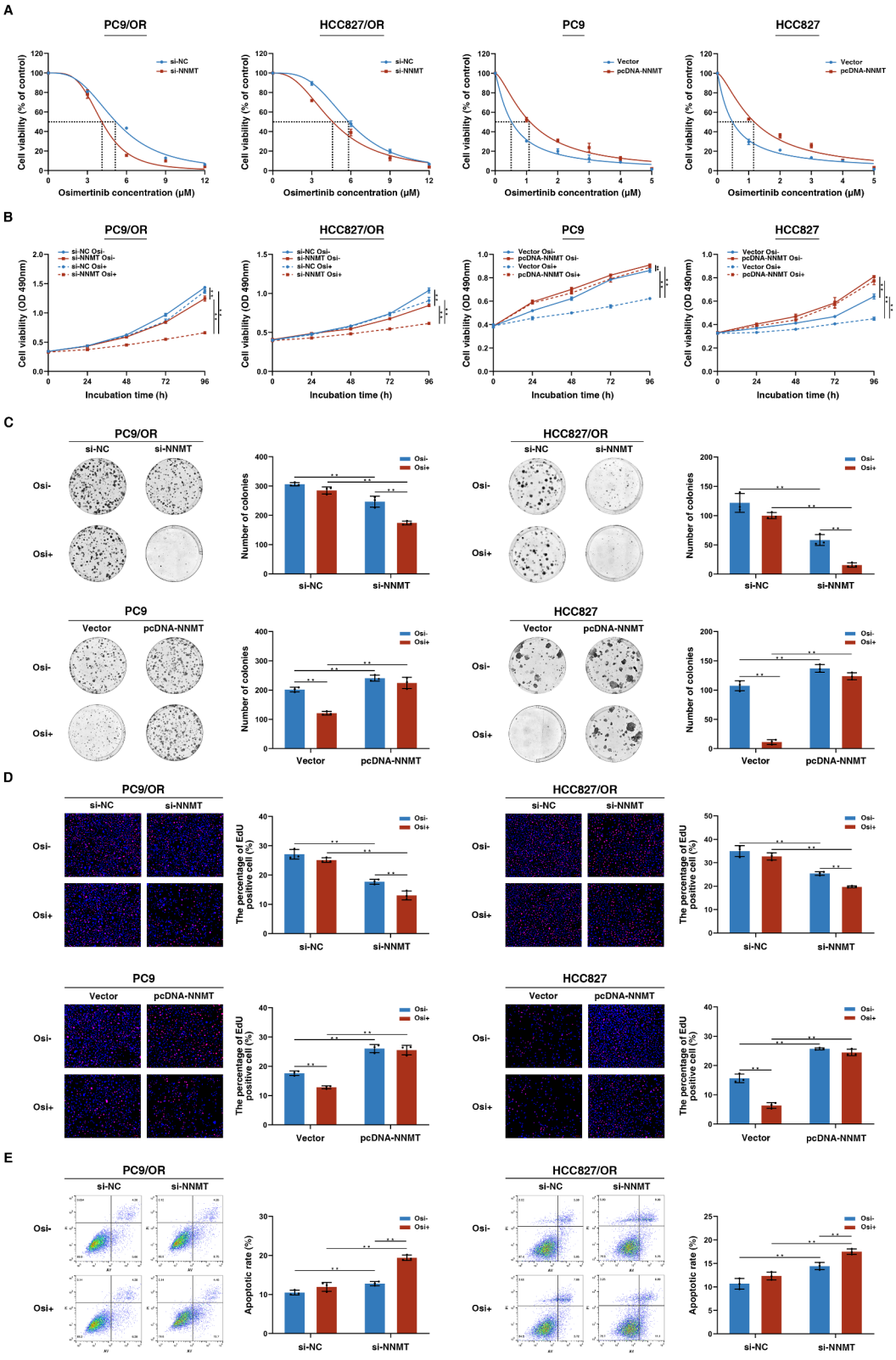

Fig. 2 NNMT regulates EGFR-TKI resistance in NSCLC cells. (**A**) The IC50 values of NNMT in cells after its knockdown or overexpression. (**B**) MTT assays were performed to determine cell viability and drug resistance after NNMT knockdown or overexpression. (**C**) Colony formation assays were used to evaluate the colony formation capacity after NNMT knockdown or overexpression. (**D**) Cell proliferation was analyzed using EdU after NNMT knockdown or overexpression. (**E**) Cell apoptosis was determined in TKI-resistant cells after NNMT knockdown. Three independent experiments were performed. $^{**}P < 0.01$

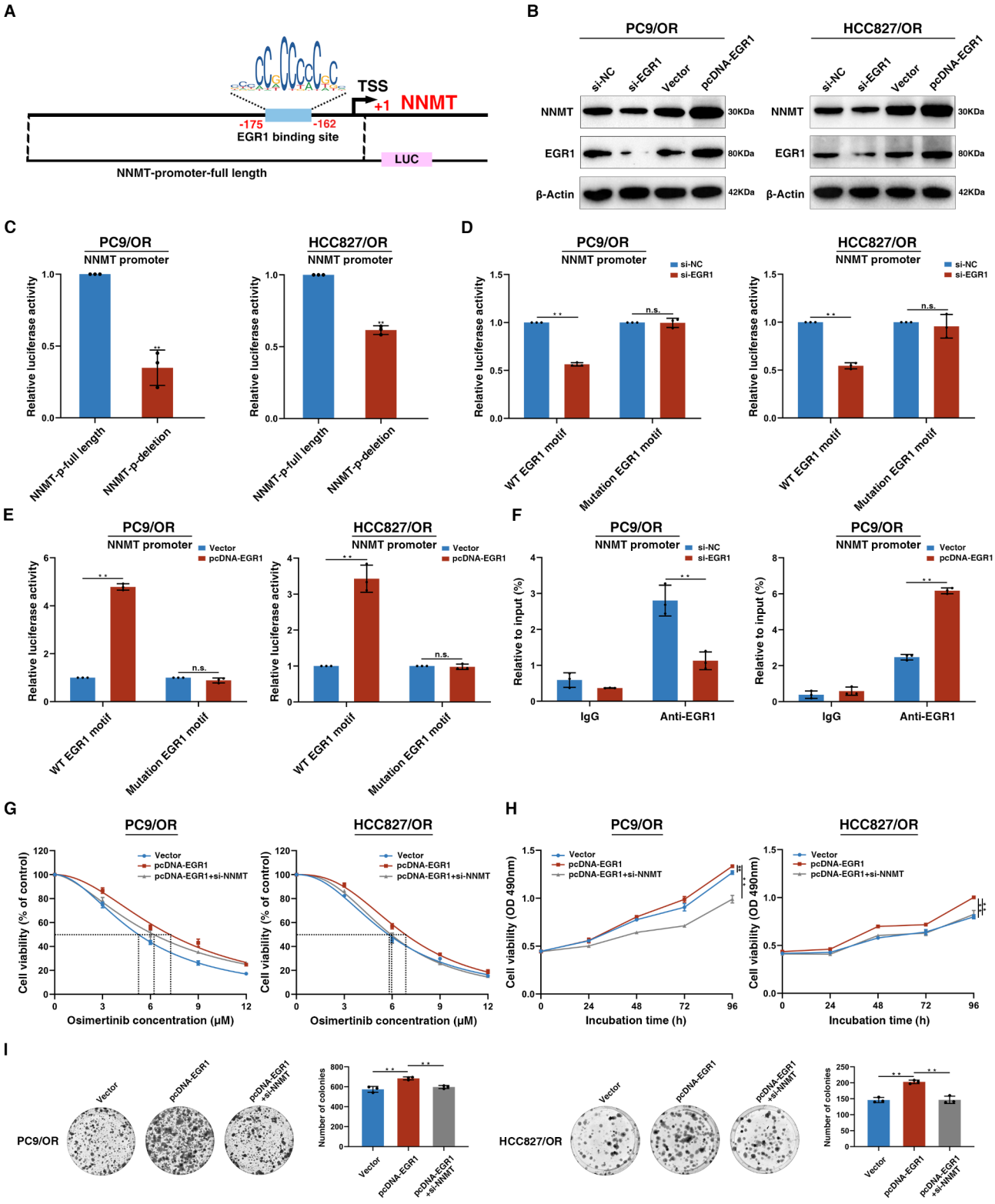

Fig. 3 EGR1 directly transcriptionally activates NNMT in TKI resistance. (**A**) Schematic diagram of the EGR1 binding site in the NNMT promoter. (**B**) NNMT expression was determined after EGR1 was knocked down or overexpressed. (**C**-**E**) NNMT promoter activity was tested using a dual-luciferase reporter assay after the corresponding treatments. (**F**) ChIP assays were performed to detect the enrichment of EGR1 in the NNMT promoter. (**G**-**I**) IC50, MTT and colony formation assays were used to determine cell proliferation and resistance to TKIs after the corresponding treatments. Three independent experiments were performed. $^{**}P < 0.01$, n.s., not significant

Figure 4

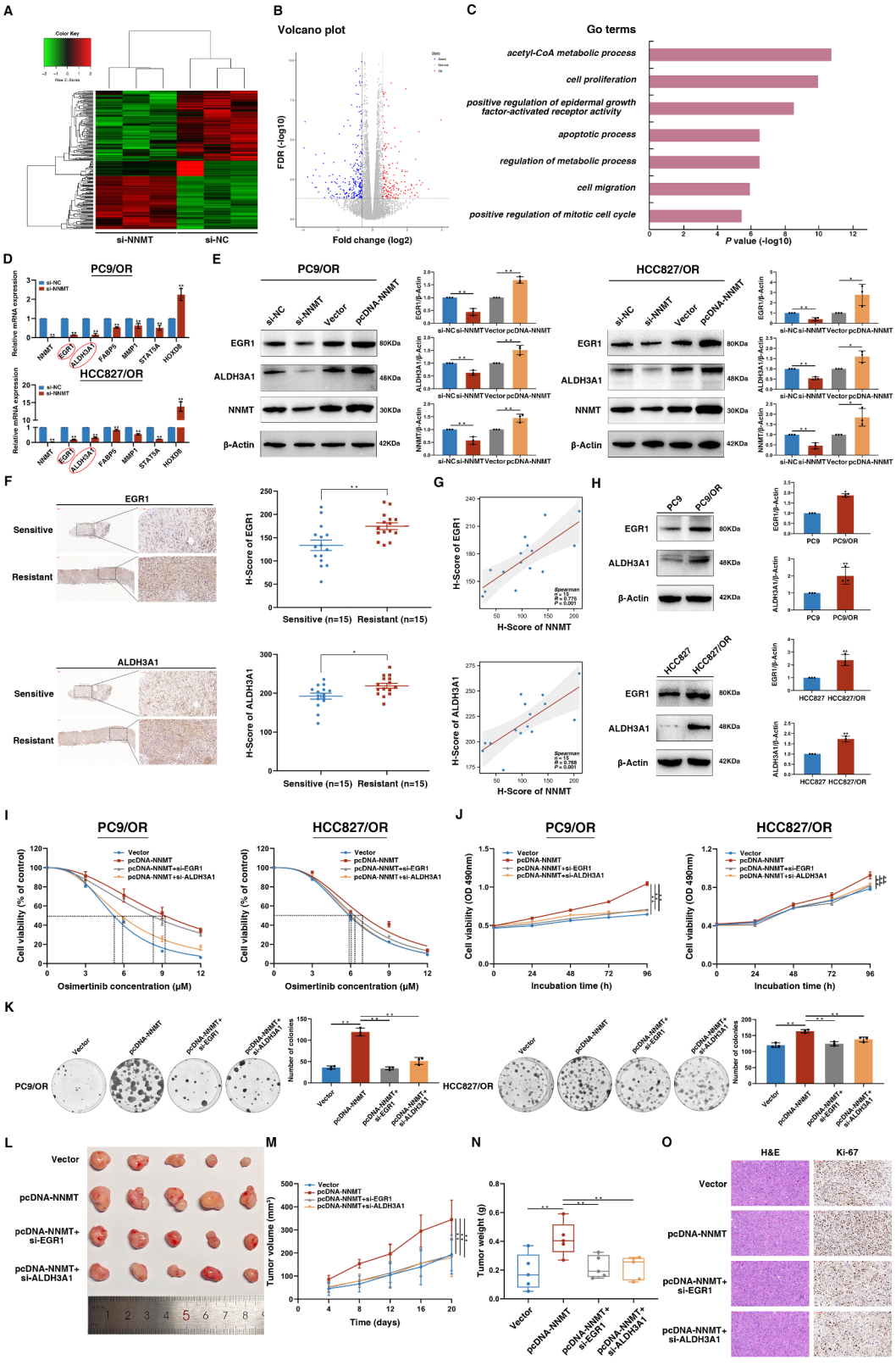

Fig. 4 (See legend on next page.)

(See figure on previous page.)

Fig. 4 NNMT regulates EGR1 and ALDH3A1, leading to the resistance of NSCLC to EGFR-TKIs. (**A**) RNA sequencing was performed to identify downstream genes after the inhibition of NNMT. (**B**) Differential gene expression was analyzed using a volcano plot. (**C**) GO analysis after NNMT knockdown. (**D**) qRT–PCR was used to verify representative genes. (**E**) Western blotting was used to detect the expression of EGR1 and ALDH3A1 after NNMT knockdown or overexpression. (**F**) EGR1 and ALDH3A1 expression was analyzed in paired tissues from TKI-sensitive and TKI-resistant patients with lung cancer. (**G**) A positive correlation between NNMT and EGR1 or ALDH3A1 in tissues from TKI-resistant patients. (**H**) EGR1 and ALDH3A1 protein expression in TKI-resistant cells and sensitive cells. (**I**-**K**) IC50, MTT and colony formation assays were used to determine cell proliferation and resistance to TKIs after the corresponding treatments. (**L**-**N**) Tumor volumes and weights were measured after the corresponding treatments. (**O**) Immunohistochemistry analysis was performed to analyze the tumor tissue. Three independent experiments were performed. $^{*}P < 0.05$, $^{**}P < 0.01$

the knockdown of NNMT in PC9/OR, HCC827/OR and HCC827/GR cells decreased EGR1 and ALDH3A1 expression, whereas NNMT overexpression increased EGR1 and ALDH3A1 expression (Fig. 4E and Figure S3A). Immunohistochemical analysis revealed that tissues from TKI-resistant lung cancer patients had higher EGR1 and ALDH3A1 levels compared with those from TKI-sensitive lung cancer patients (Fig. 4F). A positive correlation between NNMT expression and EGR1 or ALDH3A1 expression was detected in TKI-resistant tissues (Fig. 4G). Moreover, as shown in Fig. 4H and Figure S3B, EGR1 and ALDH3A1 expression levels were indeed elevated in TKI-resistant cells compared with sensitive cells. In addition, ALDEFLUOR flow cytometry revealed that TKI-resistant PC9/OR cells had higher ALDH enzyme activity than TKI-sensitive cells (Figure S3C). Moreover, treatment of PC9/OR cells with the ALDH inhibitor N, N-Diethylaminobenzaldehyde (DEAB) reduced ALDH enzymatic activity and the IC50 value of osimertinib in PC9/OR cells (Figure S3D and S3E). MTT and colony formation assays further showed that DEAB reduced the proliferation capacity of PC9/OR compared to the control group or treatment with osimertinib alone. Particularly, the combination of DEAB and osimertinib had a more pronounced effect (Figure S3F and S3G). In addition, NNMT or ALDH3A1 knockdown in PC9/OR cells decreased the proportion of $ALDH^{+}$ cells, as measured using an ALDEFLUOR flow cytometry assay (Figure S3H). We also found that ALDH3A1 promoted cell proliferation and resistance to EGFR-TKIs using MTT and colony formation assays (Figure S3I-S3K). Furthermore, EGR1 or ALDH3A1 knockdown in PC9/OR, HCC827/OR and HCC827/GR cells reversed the enhanced resistance to TKIs and the promotion of cell proliferation mediated by NNMT overexpression (Fig. 4I - K and Figure S3L-S3N). EGR1 or ALDH3A1 knockdown also reversed NNMT overexpression-mediated proliferation in vivo (Fig. 4L - O).

NNMT is involved in methyl metabolism. NNMT catalyzes the conversion of nicotinamide to 1-methyl nicotinamide by depleting S-adenosyl methionine (the methyl group donor) to generate S-adenosylhomocysteine (SAH), altering histone methylation levels [22, 29]. As shown in Fig. 5A and Figure S4A, NNMT knockdown in PC9/OR and HCC827/GR cells significantly increased SAM and SAM/SAH. Previous studies have shown that NNMT transcriptionally regulates gene expression by affecting H3K9me3 and H3K27me3 in the promoter regions of genes [22, 30]. Our Western blot analysis revealed that the knockdown of NNMT in PC9/OR, HCC827/OR and HCC827/GR cells increased H3K9me3 and H3K27me3 expression, whereas NNMT overexpression reduced H3K9me3 and H3K27me3 levels (Fig. 5B and Figure S4B). NNMT knockdown in PC9/OR, HCC827/OR and HCC827/GR cells significantly increased H3K9me3 and H3K27me3 levels and decreased EGR1 and ALDH3A1 expression (Fig. 5C and D and Figure S4C-S4D), whereas treatment with the H3K9me3 and H3K27me3 inhibitors BIX-01294 and GSK-J1 [31, 32] reversed these effects (Fig. 5C and D and Figure S4C-S4D). To further explore the regulatory mechanism of NNMT-mediated histone methylation, SAM or methionine was added to the cell culture medium to restore the intracellular methylation levels (Fig. 5E and Figure S4E). We found that NNMT overexpression repressed H3K9me3 and H3K27me3 levels and induced the expression of EGR1 or ALDH3A1. Treatment with SAM or methionine reversed the increase in H3K9me3 and H3K27me3 levels and inhibited EGR1 and ALDH3A1 expression in PC9/OR, HCC827/OR and HCC827/GR cells (Fig. 5E and Figure S4E). Furthermore, a ChIP experiment revealed that NNMT knockdown significantly increased H3K9me3 and H3K27me3 levels in the promoters of EGR1 and ALDH3A1, whereas the overexpression of NNMT had the opposite effect in both PC9/OR and HCC827/GR cells (Fig. 5F and G and Figure S4F-S4I). These data indicate that NNMT promotes EGR1 and ALDH3A1 expression via H3K9me3 and H3K27me3.

NNMT mediates histone lactylation to generate a lactate-mediated positive feedback loop leading to TKI resistance

ALDH3A1 is an NAD^{+}-dependent enzyme that oxidizes various endogenous and exogenous aldehydes to carboxylic acids [33, 34]. ALDH3A1 enhances the uptake of glucose and glycolytic processes by activating the LDHA pathway, causing lactic acid secretion and thus promoting cancer cell proliferation [33]. To test whether NNMT regulates glycolysis via ALDH3A1, we conducted an ECAR assay to detect the glycolytic capacity of PC9/OR and HCC827/GR cells. As shown in Fig. 6A and Figure S5A, the knockdown of NNMT in TKI-resistant cells inhibited

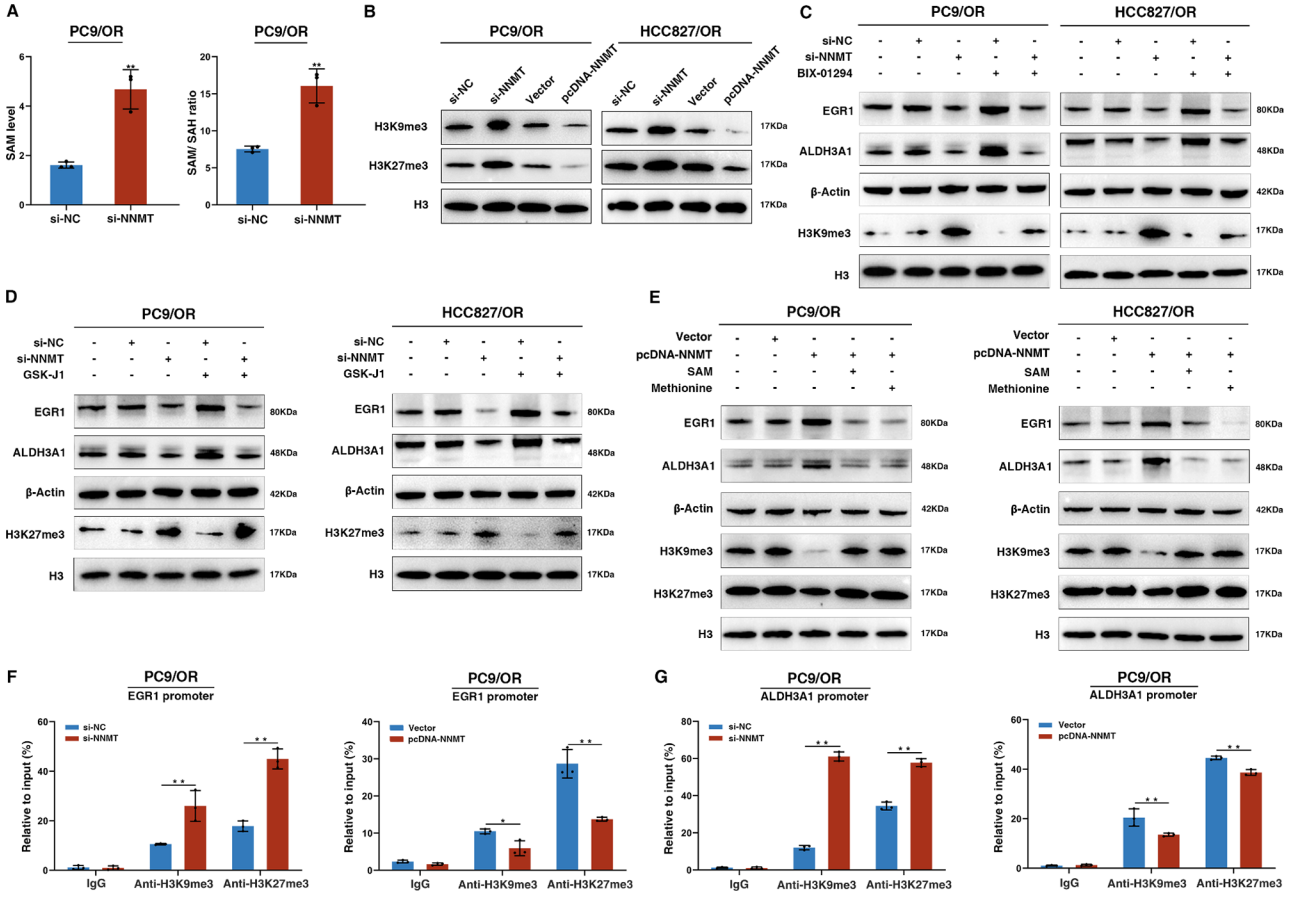

Fig. 5 NNMT reduces H3K9me3 and H3K27me3, leading to epigenetic activation of EGR1 and ALDH3A1 and resistance of NSCLC to EGFR-TKIs. (**A**) SAM and SAM/SAH were increased after NNMT knockdown in PC9/OR cells. (**B**) Western blot assays were used to detect the expression of H3K9me3 and H3K27me3 after NNMT knockdown or overexpression. (**C**-**E**) Western blot assays for the corresponding treatments. (**F**) ChIP assays showing the levels of H3K9me3 and H3K27me3 modifications in the EGR1 promoter after NNMT knockdown or overexpression. (**G**) ChIP assays showing the levels of H3K9me3 and H3K27me3 modifications in the promoter of ALDH3A1 after NNMT knockdown or overexpression. Three independent experiments were performed. $^{*}P < 0.05$, $^{**}P < 0.01$

glycolysis. The overexpression of ALDH3A1 reversed the inhibition of glycolysis caused by NNMT knockdown (Fig. 6A and Figure S5A). Moreover, NNMT knockdown in PC9/OR and HCC827/GR cells significantly decreased lactate and ATP levels compared with those in the control cells (Fig. 6B and C and Figure S5B-S5C). ALDH3A1 overexpression reversed the reduced lactate and ATP levels caused by NNMT knockdown (Fig. 6B and C and Figure S5B-S5C). Recently, lactate-derived histone lysine lactylation was identified as a newly discovered epigenetic modification that activates gene transcription from chromatin [35, 36]. Lactylation can affect various pathophysiological processes, including tumorigenesis [35–37]. Interestingly, our Western Blot analysis revealed that NNMT expression in PC9/OR, HCC827/OR and HCC827/GR cells was significantly increased after treatment with 5–20 μM lactic acid (Fig. 6D and Figure S5D). Because NNMT promotes lactate production, we infer that increased lactic acid levels could induce histone lysine lactylation, thereby altering NNMT expression. Our Western blot assays revealed that the predominant band of lactylated proteins was approximately 17 kDa (Fig. 6E). Therefore, we investigated whether the induction of NNMT could be caused by H3K18la. We found that lactic acid increased H3K18la and pan-Kla expression in PC9/OR, HCC827/OR and HCC827/GR cells, suggesting that histone lactylation plays a regulatory role in TKI resistance (Fig. 6E and Figure S5E). Indeed, immunofluorescence and immunohistochemistry assays revealed that tissues from TKI-resistant patients presented higher levels of global lactylation than those from TKI-sensitive patients did, and the lactylated proteins (red) were located mainly in the nucleus (Fig. 6F and G). Moreover, pan-Kla expression levels were positively correlated with NNMT expression (Fig. 6H). H3K18la levels were similar to those in TKI-sensitive patients in terms of global lactylation in tissues from TKI-resistant patients (Fig. 6I - K). In addition, TKI-resistant cells presented increased pan-Kla and H3K18la expression compared with TKI-sensitive cells (Fig. 6L and Figure S5F).

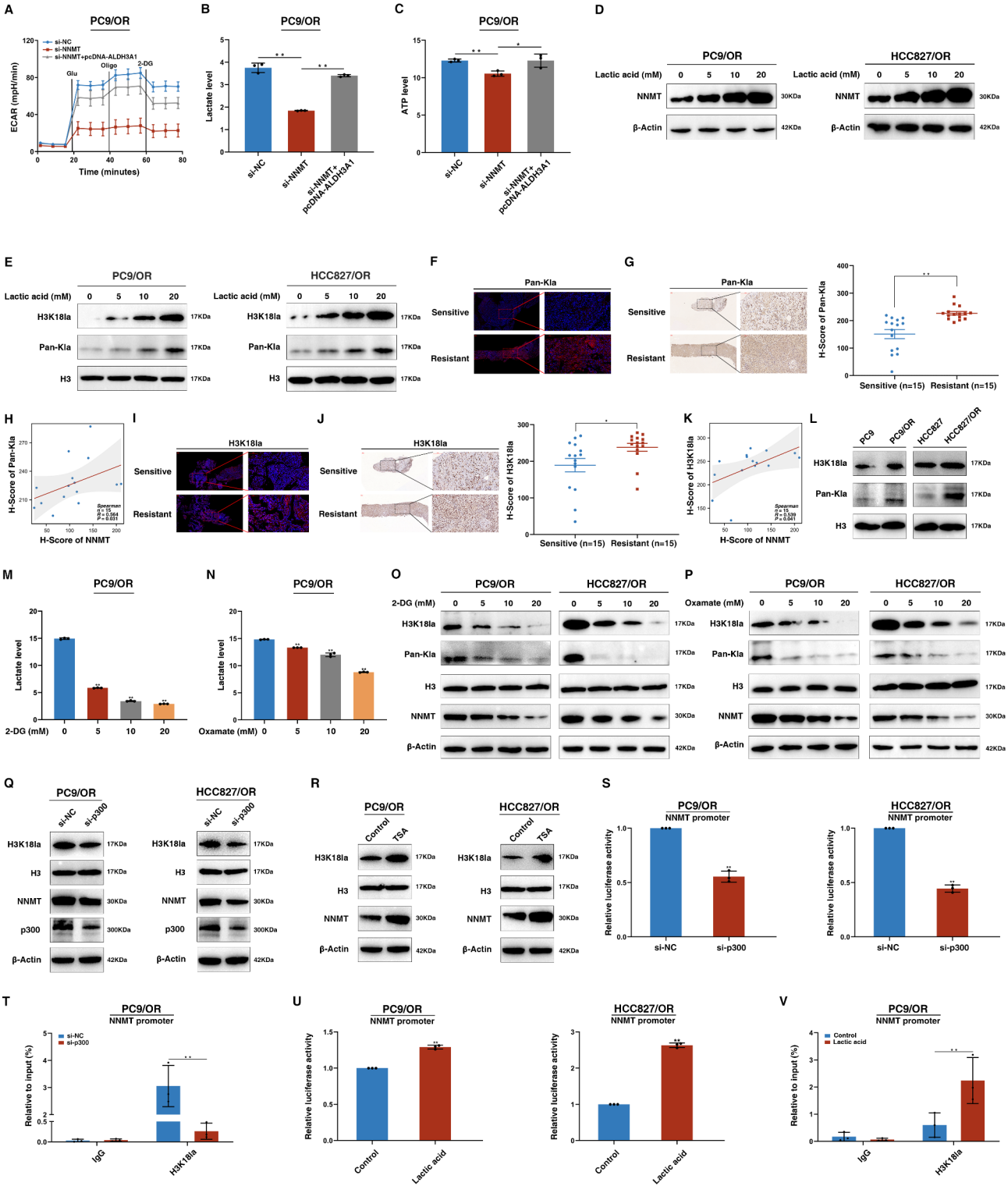

Fig. 6 (See legend on next page.)

Furthermore, glycolysis inhibitors (2-DG or oxamate) decreased lactate production in a dose-dependent manner (Fig. 6M and N and S5G-S5H). Moreover, the expression levels of pan-Kla, H3K18la and NNMT markedly decreased with increasing concentrations of glycolysis inhibitors (Fig. 6O and P and Figure S5I-S5J). The acetyltransferase p300 has been identified as a potential histone Kla "writer" enzyme, and histone deacetylase (HDAC)

(See figure on previous page.)

Fig. 6 ALDH3A1 mediates histone lactylation by targeting NNMT to promote EGFR-TKI resistance. (**A**) Glycolysis capacity was measured in resistant cells after the corresponding treatments. (**B**, **C**) The levels of lactate and ATP were detected in resistant cells after the corresponding treatments. (**D**) Western blot analysis of lactic acid-treated cells. (**E**) Expression of pan-Kla and H3K18la following lactic acid treatment. (**F**, **G**) Increased level of global lactylation in tissues from TKI-resistant patients and lactated proteins (red) located in the nucleus. (**H**) The expression of pan-Kla was positively correlated with NNMT. (**I**, **J**) H3K18la levels were greater in tissues from TKI-resistant patients than in those from TKI-sensitive patients. (**K**) H3K18la expression was positively correlated with NNMT. (**L**) Pan-Kla and H3K18la levels were increased in TKI-resistant cells. (**M**, **N**) Glycolysis inhibitors (2-DG or oxamate) decreased lactate levels in a dose–dependent manner. (**O**, **P**) The expression of pan-Kla, H3K18la and NNMT was determined after the corresponding treatments. (**Q**) Western blot assays were used to detect H3K18la, NNMT and p300 expression after p300 was knocked down. (**R**) Western blot assays detected H3K18la and NNMT expression after treatment with the HDAC inhibitor trichostatin A (TSA). (**S**) Luciferase reporter assays after p300 knockdown. (**T**) ChIP assay after p300 knockdown. **(U)** Luciferase reporter assay after treatment with lactic acid. (**V**) ChIP assay after treatment with lactic acid. Three independent experiments were performed. $^{*}P < 0.05$, $^{**}P < 0.01$

1–3 are regarded as histone lysine delactylases [37, 38]. We found that p300 knockdown markedly decreased the expression of NNMT and H3K18la (Fig. 6Q and Figure S5K). In addition, the HDAC inhibitor trichostatin A (TSA) increased histone lactylation and NNMT expression (Fig. 6R and Figure S5L). A luciferase reporter assay revealed that the NNMT promoter activity decreased after p300 was knocked down (Fig. 6S and Figure S5M). Chromatin immunoprecipitation (ChIP) further demonstrated that the knockdown of p300 inhibited the binding of H3K18la to the NNMT promoter (Fig. 6T and Figure S5N). Furthermore, a luciferase reporter assay revealed that lactic acid increased NNMT promoter activity (Fig. 6U and Figure S5O), and a ChIP assay revealed that H3K18la directly bound to the NNMT promoter. Lactate treatment significantly increased the enrichment of H3K18la in the NNMT promoter (Fig. 6V and Figure S5P). These data indicate that histone lysine lactylation represents a novel mechanism underlying the activation of NNMT in TKI resistance in lung cancer.

We further found that ALDH3A1 knockdown reduced the expression of pan-Kla, H3K18la and NNMT, whereas ALDH3A1 overexpression had the opposite effect (Fig. 7A and Figure S6A). Moreover, an ECAR assay revealed that the knockdown of ALDH3A1 reduced glycolytic ability in TKI-resistant cells and that the overexpression of NNMT partially reversed this inhibitory effect (Fig. 7B and Figure S6B). Similarly, the overexpression of NNMT reversed the decreased levels of lactate and ATP caused by the knockdown of ALDH3A1 (Fig. 7C and D and Figure S6C-S6D). Importantly, NNMT promoter activity decreased or increased after knockdown or overexpression ALDH3A1, respectively, and NNMT promoter activity was also repressed or enhanced by the knockdown or overexpression of NNMT itself, respectively (Fig. 7E - H and Figure S6E). Moreover, ALDH3A1 knockdown partially reversed the increase in the promoter activity of NNMT caused by the overexpression of NNMT (Fig. 7I and J and Figure S6F). In addition, ChIP assays revealed that ALDH3A1 knockdown inhibited the binding of H3K18la to the NNMT promoter and that NNMT overexpression reversed this inhibitory effect (Fig. 7K and Figure S6G).

IC50, MTT and colony formation assays revealed that the knockdown of NNMT in PC9/OR, HCC827/OR and HCC827/GR cells partially reversed the TKI resistance and cell proliferation mediated by ALDH3A1 overexpression (Fig. 7L - N and Figure S6H-S6J). Moreover, treatment with lactic acid reversed the increased TKI sensitivity and inhibited cell proliferation mediated by ALDH3A1 knockdown (Fig. 7O - Q and Figure S6K-S6M). These data suggest that NNMT and ALDH3A1 constitute a lactate-mediated positive lactylation regulatory loop in TKI resistance. Moreover, the dual-luciferase reporter gene assay results indicated that EGR1 knockdown reversed the increase in NNMT promoter activity, which was induced by NNMT overexpression (Fig. 7R and Figure S6N). In addition, a ChIP assay demonstrated that NNMT overexpression increased the binding abundance of EGR1 to the NNMT promoter, whereas knockdown of EGR1 reversed this promoting effect (Fig. 7S and Figure S6O).

NNMT regulates EGFR-TKI resistance in lung cancer in vivo

To elucidate the role of NNMT in EGFR-TKI resistance in vivo, PC9/OR cells stably transfected with sh-NNMT were injected into nude mice. When palpable tumors were detected, the mice were treated daily with osimertinib (25 mg/kg) or saline (control) via oral gavage. As shown in Fig. 8A - D, NNMT knockdown reduced the tumor growth rate, tumor volume, and tumor weight. Immunohistochemical staining of xenograft tumor tissues revealed that NNMT knockdown led to decreased Ki67, NNMT, EGR1 and ALDH3A1 expression (Fig. 8E).

To further evaluate the therapeutic potential of NNMT in TKI resistance, we used NNMTi, a small-molecule NNMT inhibitor [22], and found that NNMTi suppressed tumor growth in a osimertinib-resistant xenograft model, suggesting its therapeutic potential (Figure S7A-S7C). PC9/OR cells were subcutaneously injected into nude mice, which were randomly divided into four groups: control, osimertinib, NNMTi, and osimertinib plus NNMTi. Compared with the control group or treatment with osimertinib alone, treatment with NNMTi reduced tumor size, and combination treatment with osimertinib and NNMTi was more effective (Fig. 8F - I).

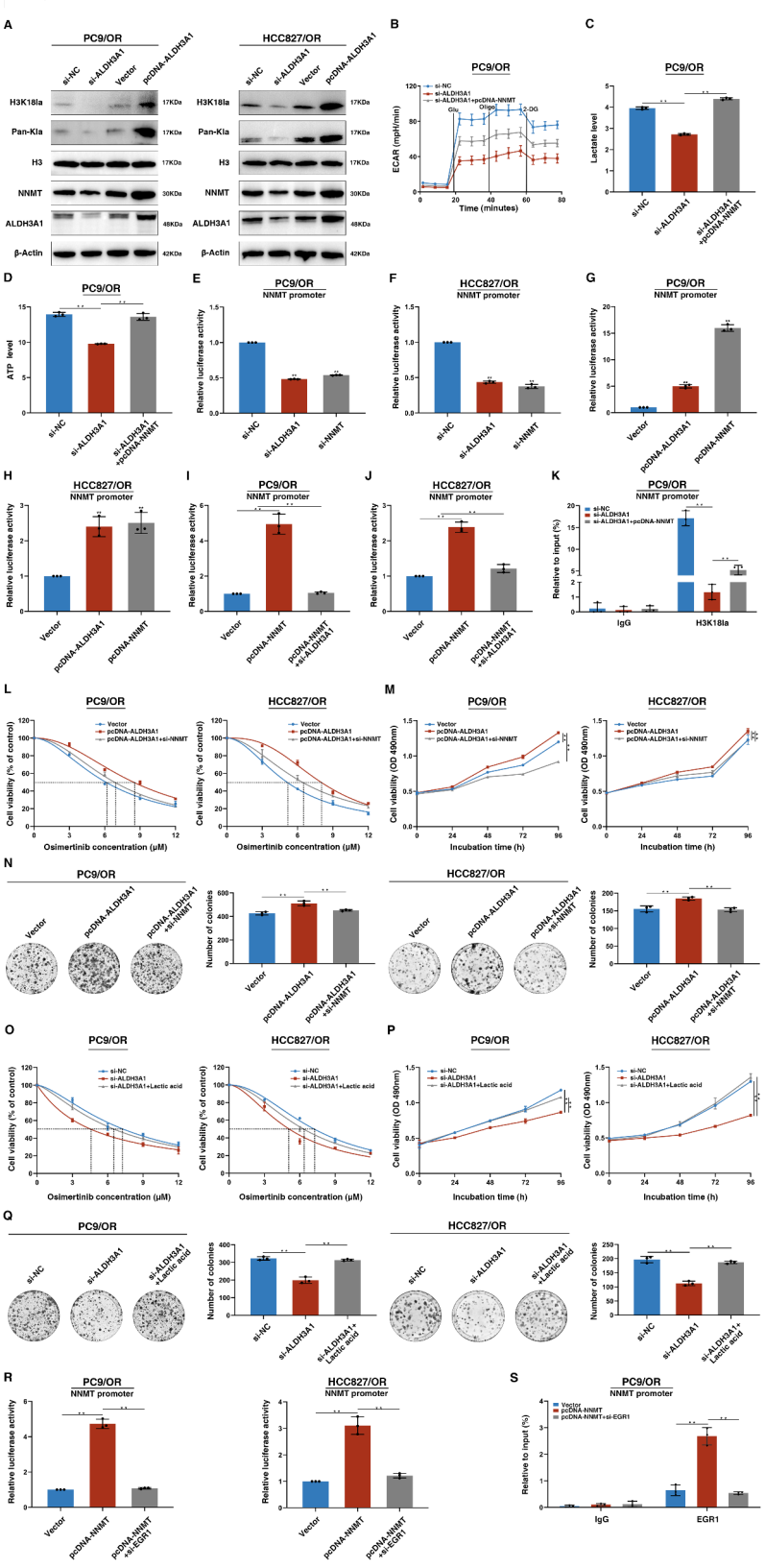

Fig. 7 (See legend on next page.)

(See figure on previous page.)

Fig. 7 NNMT promotes TKI resistance by mediating histone lactylation to generate a lactate-mediated positive feedback loop. (**A**) Western blot assays after knockdown or overexpression of ALDH3A1. (**B**) Glycolysis capacity was measured in resistant cells after the corresponding treatments. (**C**, **D**) Lactate and ATP levels were detected in resistant cells after the corresponding treatments. (**E**-**J**) NNMT promoter activity was tested using a dual-luciferase reporter gene assay after the corresponding treatments. **(K)** ChIP assay after the corresponding treatments. (**L–N**) IC50, MTT and colony formation assays were used to determine cell proliferation and resistance to TKIs after the corresponding treatments. (**O–Q**) IC50, MTT and colony formation assays were used to determine cell proliferation and resistance to TKIs after the corresponding treatments. (**R**) Dual-luciferase reporter assays after the corresponding treatments. (**S**) ChIP assays after the corresponding treatments. Three independent experiments were performed. $^{**}P < 0.01$

Immunohistochemical analysis revealed that compared with control treatment, combination treatment with osimertinib and NNMTi decreased Ki67, NNMT, EGR1 and ALDH3A1 expression (Fig. 8J). Moreover, in vitro cell viability assays also supported the above findings in vivo (Figure S7D-S7F).

To further evaluate the therapeutic potential of targeting NNMT in the NNMT/EGR1/ALDH3A1 regulatory axis in TKI resistance, we performed in vitro and in vivo experiments. Compared with the control, overexpression of EGR1 or ALDH3A1 promoted tumor growth in vivo. Furthermore, EGR1 or ALDH3A1 overexpression-promoted tumor growth was reversed by treatment with NNMTi (Fig. 8K - N). Immunohistochemical results revealed that EGR1 or ALDH3A1 overexpression increased Ki67 expression (Fig. 8O). NNMTi reversed the expression of Ki67 induced by the overexpression of EGR1 or ALDH3A1 (Fig. 8O). Our in vitro MTT and colony formation assays revealed similar blocking effects of NNMTi (Figure S7G-S7J). Taken together, our data imply that NNMT is a potentially effective therapeutic target for TKI resistance in lung cancer.

Discussion

EGFR-TKIs significantly improve the survival of patients with EGFR-TKI sensitive mutations. The mechanism of acquired resistance to EGFR-TKIs is complex and requires further in-depth investigation. To date, the key genes involved in cancer development have been identified with distinct histone modification patterns due to abnormal transcriptome features in tumorigenesis and drug resistance [12]. NNMT belongs to the N-methyltransferase family, which can regulate the epigenetic state of histone methylation of target genes. Many studies have shown that NNMT is closely related to the progression and drug resistance of cancers and is overexpressed in a variety of tumors, and NNMT has been shown to promote the survival of cancer cells [22, 23, 39]. However, the activation and detailed functional mechanisms of NNMT in TKI resistance in lung cancer remain largely unknown. In this study, we revealed the critical role of the NNMT-mediated dual positive feedback loop in driving acquired EGFR-TKI resistance in NSCLC. We discovered that EGR1-mediated transcriptional activation contributed to NNMT upregulation in TKI resistance. EGR1 is a well-known transcription factor involved in tumorigenesis and drug resistance [26, 27, 40]. For example, EGR1-mediated metabolic reprogramming contributes to ibrutinib resistance in B-cell lymphoma [27]. In addition, we revealed a novel mechanism of NNMT activation at the epigenetic level. Our study revealed that lactic acid increases H3K18la levels in the NNMT promoter to promote NNMT expression. The increase in histone lactylation in promoter regions induces the expression of genes associated with tumorigenesis and drug resistance [36, 37, 41]. For example, histone lactylation activated RUBCNL expression, thereby promoting the resistance of colorectal cancer to bevacizumab [41]. Here, we report for the first time that histone lactylation drives NNMT expression and accelerates TKI resistance. A previous study revealed that NNMT promotes EGFR-TKI resistance in lung cancer by increasing c-Myc expression [42]. Yao et al. revealed that c-Myc directly binds the EGR1 promoter and transcriptionally activates EGR1 [43]. These studies indicate that c-Myc is potentially involved in the EGR1/NNMT/EGR1 loop by transcriptionally activating EGR1 to promote TKI resistance in lung cancer. In addition, Bach DH et al. reported that NNMT promotes TKI resistance by activating AKT in lung cancer [44]. ALDH3A1 may be involved in activating the AKT oncogenic signaling pathway in lung cancer [45]. AKT pathway activation facilitates lactate production in lung cancer [46, 47]. These findings indicate that AKT might be involved in lactate production by communicating with ALDH3A1 and thereby participating in the NNMT/ALDH3A1/lactate/NNMT loop to promote TKI resistance in lung cancer.

NNMT, a methyltransferase, participates in histone methylation by regulating SAM methylation metabolism [22, 29, 30]. For example, NNMT promotes cholangiocarcinoma progression by inhibiting the level of histone lysine methylation to activate the EGFR/STAT3 pathway [30]. NNMT decreases H3K27me3 levels and then activates WNT signaling to promote the progression of early gastric cardia adenocarcinoma [22]. Our present study revealed that NNMT could be a powerful modifier of histone methylation in TKI resistance in lung cancer. High NNMT expression epigenetically activates EGR1 and ALDH3A1 by reducing H3K27me3 and H3K9me3 levels in the promoters of EGR1 and ALDH3A1. Given that EGR1 transcriptionally activates NNMT, a positive feedback loop of EGR1/NNMT/EGR1 could promote TKI resistance in lung cancer.

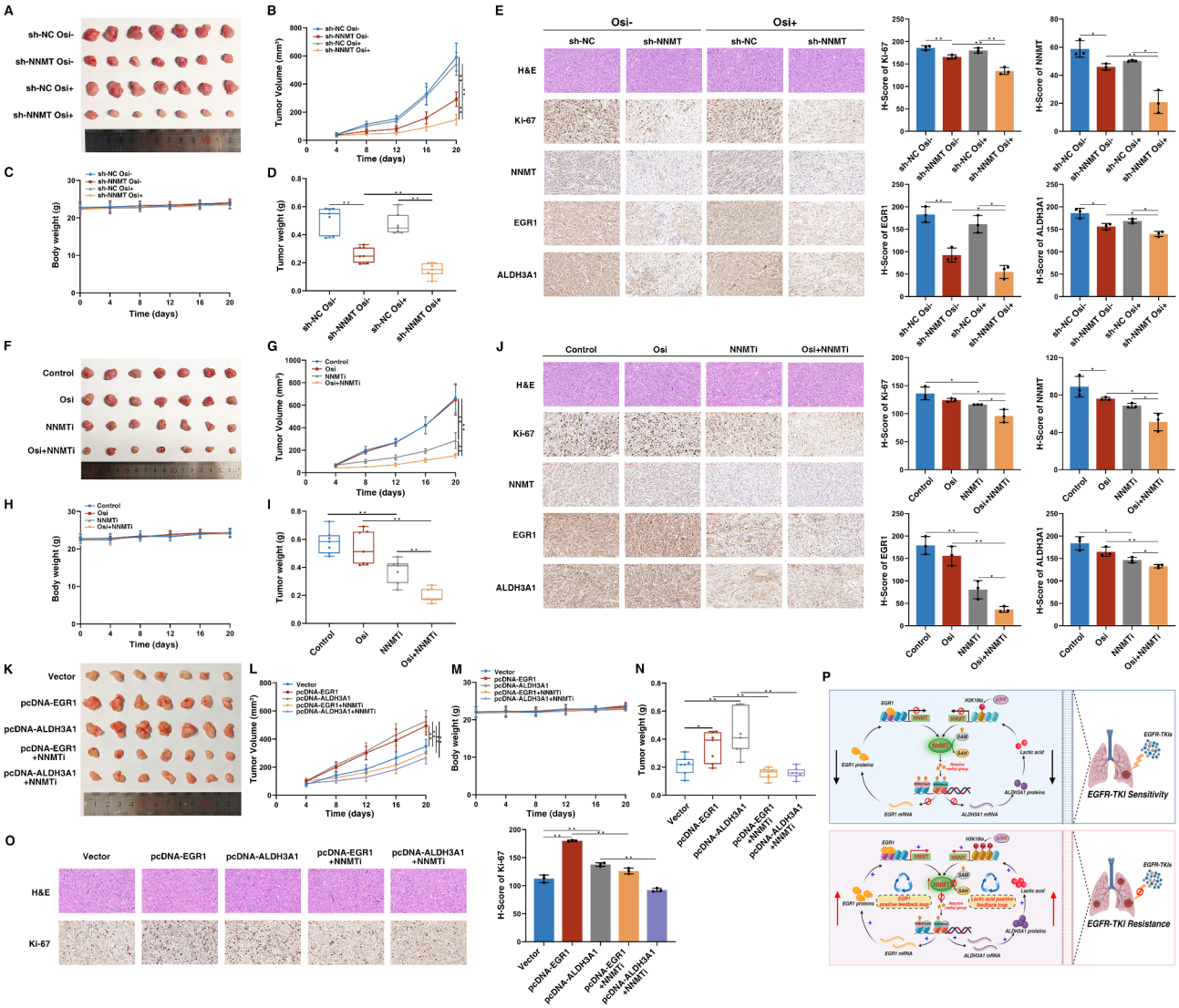

Fig. 8 NNMT regulates EGFR-TKI resistance in lung cancer in vivo. (**A**) Tumor tissues from mice. (**B**) Tumor volumes were calculated at regular intervals 4 days after injection. (**C**) Mouse body weights were measured at regular intervals of 4 days. (**D**) Tumor weights are presented as the means ± SD (standard deviation). (**E**) The tumor sections were subjected to immunohistochemistry (IHC) staining for H&E, Ki67, NNMT, EGR1 and ALDH3A1. (**F**) Tumor tissue from the mice. (**G**) Tumor volumes were calculated at regular intervals 4 days after injection. (**H**) Mouse body weights were measured. **(I)** Tumor weights are presented as the means ± SD. (**J**) The tumor sections were subjected to immunohistochemical staining. **(K)** Tumor tissues from the mice. (**L**) Tumor volumes were calculated at regular intervals of 4 days after injection. (**M**) Mouse body weights were measured. (**N**) Tumor weights are presented as the means ± SD. (**O**) Tumor sections were subjected to immunohistochemical staining. (**P**) Proposed mechanisms for NNMT-mediated EGFR-TKI resistance in NSCLC. $^{*}P < 0.05$, $^{**}P < 0.01$

Lactate is an important intermediary product in metabolic processes and plays critical roles in various diseases, including cancer [35–37, 48]. Lactate accumulated in tumor cells can bind to lysine residues in proteins to promote lactate modification. An increasing amount of evidence suggests that lactylation has important functions in gene expression, especially in histone lactylation [21, 41]. Histone lysine lactylation is a newly characterized epigenetic modification that can directly interact with chromatin to regulate transcription [35]. Here, lactate serves as a substrate to generate lactyl-CoA for lysine lactylation on histones to regulate gene expression in diverse pathophysiological conditions, including cancer. In addition, lactic acid levels are closely related to tumor resistance. Previous studies have confirmed that compared with sensitive cells, drug-resistant cells present higher basal metabolic levels and lactic acid contents [49]. Our data also revealed elevated lactate levels in TKI-resistant lung cancer cells. NNMT is widely regarded as an important metabolic-epigenetic enzyme. Many studies

have revealed that NNMT serves as a master metabolic regulator in tumorigenesis [29, 50]. For example, NNMT depletion leads to intracellular glutamine accumulation, which has negative effects on mitochondrial function and survival in clear cell renal cell carcinoma [50]. Xie et al. reported that 1-MNA decreases ROS levels, alters the NAD^+/NADH ratio, and increases intracellular ATP levels, suggesting that NNMT maintains cancer cell growth by affecting energy metabolism [51]. However, the role of NNMT in lactylation remains unclear. In addition, the role of lactylation modification in the TKI resistance of lung cancer also needs to be clarified. We first revealed that NNMT activates ALDH3A1 through histone methylation to promote lactate production and that high levels of lactate, in turn, epigenetically activate NNMT expression through histone lactylation (H3K18la) to generate a lactate-mediated positive regulatory loop (NNMT/ALDH3A1/lactate/NNMT) that is dependent on NNMT in the context of TKI resistance in lung cancer. Previous studies also revealed that ALDH3A1 promotes the glycolytic process by activating the LDHA pathway, causing lactic acid secretion and thus accelerating cell proliferation. This mechanism is involved in tumorigenesis and drug resistance [33, 34, 52]. In addition, the expression of p300, a "writer" of lactylation in the NNMT promoter, is activated in this lactylation modification process. Our study is recognized as an important contribution to the current body of knowledge on the relationship between metabolism-epigenetics and drug resistance in tumors. This highly efficient NNMT-mediated histone lactylation provides a novel perspective for understanding the molecular mechanism of TKI resistance in lung cancer.

We also investigated the therapeutic potential of NNMT in vivo. We found that combination treatment with a small-molecule inhibitor (NNMTi) and osimertinib exhibited excellent antitumor efficacy. These results suggest that targeting NNMT may represent an effective therapeutic strategy to overcome TKI resistance in NSCLC.

Conclusions

Our findings clarify the NNMT-mediated dialog between histone methylation and histone lactylation, providing new insights into epigenetic regulation in the TKI resistance of NSCLC (Fig. 8P). More importantly, our study indicates that the epigenetic modification of histones plays a crucial role in TKI-resistant NSCLC and that NNMT inhibitors are potential therapeutic agents for overcoming TKI resistance in NSCLC.

Supplementary Information

The online version contains supplementary material available at https://doi.org/10.1186/s12943-025-02285-y.

Supplementary Material 1

Supplementary Material 2

Acknowledgements
The authors thank NovelBioinformatics Ltd., Co. for the support of bioinformatics analysis with their NovelBrain Cloud Analysis Platform (www.novelbrain.com).

Author contributions
Conception and design: EBZ. Development of methodology: JLD, XYL and CZ. Acquisition of data: JLD, XYL, CZ and TYQ. Analysis of data: JLD, TYQ and JS. Writing, review, and revision of manuscript: JLD and EBZ. Administrative, technical, or material support: WL, PPW, RHG, DDY, LH and EBZ.

Funding
This work was supported by National Natural Science Foundation of China [82472672, 82172992, 82472672, 82172982, 82403029, 82273171 and 82103133] and Jiangsu Province Science and Technology Project [BK20211253, BK20231156 and BK20210973]. This work was also supported by Jiangsu Province Excellent Postdoctoral Program [2023ZB419], China Postdoctoral Science Foundation [2023M740371], Yishan Research Project of Jiangsu Cancer Hospital [YSPY202406] and Key Project of Medical Research of the Health Commission of Jiangsu Province [K2024045].

Data availability
No datasets were generated or analysed during the current study.

Declarations

Ethics approval and consent to participate
The study was approved by the Ethics Committee on Human Research of the First Affiliated Hospital of Nanjing Medical University, and it was performed in compliance with the Helsinki Declaration. All patients have given written informed consent for publication.

Consent for publication
Not applicable.

Competing interests
The authors declare no competing interests.

Author details
[1]Department of Oncology, First Affiliated Hospital of Nanjing Medical University, Nanjing, Jiangsu, PR China
[2]Department of Epidemiology, Center for Global Health, School of Public Health, Nanjing Medical University, Nanjing 211166, China
[3]Department of Oncology, Xinhua Hospital, Shanghai Jiaotong University School of Medicine, Shanghai, PR China
[4]Clinical Research Center, The Second Hospital of Nanjing, Nanjing University of Chinese Medicine, Zhong Fu Road, Gulou District, Nanjing, Jiangsu 210003, PR China
[5]Department of Oncology, Jiangsu Cancer Hospital, The Affiliated Cancer Hospital of Nanjing Medical University, Jiangsu Institue of Cancer Research, Nanjing, Jiangsu, PR China
[6]Department of Oncology, Xuzhou Central Hospital, Xuzhou School of Clinical Medicine of Nanjing Medical University, Xuzhou, Jiangsu, PR China
[7]Jiangsu Key Lab of Cancer Biomarkers, Prevention and Treatment, Collaborative Innovation Center for Cancer Personalized Medicine, Nanjing Medical University, Nanjing 211166, China

Received: 9 October 2024 / Accepted: 26 February 2025
Published online: 15 March 2025

References

1. Siegel RL, Giaquinto AN, Jemal A. Cancer statistics, 2024. CA Cancer J Clin. 2024;74(1):12–49.

2. Bender E. Epidemiology: the dominant malignancy. Nature. 2014;513(7517):S2–3.
3. Maemondo M, Inoue A, Kobayashi K, Sugawara S, Oizumi S, Isobe H, Gemma A, Harada M, Yoshizawa H, Kinoshita I, et al. Gefitinib or chemotherapy for non-small-cell lung cancer with mutated EGFR. N Engl J Med. 2010;362(25):2380–8.
4. Soria JC, Ohe Y, Vansteenkiste J, Reungwetwattana T, Chewaskulyong B, Lee KH, Dechaphunkul A, Imamura F, Nogami N, Kurata T, et al. Osimertinib in untreated EGFR-Mutated advanced Non-Small-Cell lung Cancer. N Engl J Med. 2018;378(2):113–25.
5. Herbst RS, Wu YL, John T, Grohe C, Majem M, Wang J, Kato T, Goldman JW, Laktionov K, Kim SW, et al. Adjuvant osimertinib for resected EGFR-Mutated stage IB-IIIA Non-Small-Cell lung cancer: updated results from the phase III randomized ADAURA trial. J Clin Oncol. 2023;41(10):1830–40.
6. Remon J, Steuer CE, Ramalingam SS, Felip E. Osimertinib and other third-generation EGFR TKI in EGFR-mutant NSCLC patients. Ann Oncol. 2018;29(suppl1):i20–7.
7. Sun L, Zhang H, Gao P. Metabolic reprogramming and epigenetic modifications on the path to cancer. Protein Cell. 2022;13(12):877–919.
8. Zhao Z, Shilatifard A. Epigenetic modifications of histones in cancer. Genome Biol. 2019;20(1):245.
9. Deng S, Zhang J, Su J, Zuo Z, Zeng L, Liu K, Zheng Y, Huang X, Bai R, Zhuang L, et al. RNA m(6)A regulates transcription via DNA demethylation and chromatin accessibility. Nat Genet. 2022;54(9):1427–37.
10. Fatma H, Maurya SK, Siddique HR. Epigenetic modifications of c-MYC: role in cancer cell reprogramming, progression and chemoresistance. Semin Cancer Biol. 2022;83:166–76.
11. Lin Z, Li J, Zhang J, Feng W, Lu J, Ma X, Ding W, Ouyang S, Lu J, Yue P, et al. Metabolic reprogramming driven by IGF2BP3 promotes acquired resistance to EGFR inhibitors in Non-Small cell lung Cancer. Cancer Res. 2023;83(13):2187–207.
12. Baratchian M, Tiwari R, Khalighi S, Chakravarthy A, Yuan W, Berk M, Li J, Guerinot A, de Bono J, Makarov V, et al. H3K9 methylation drives resistance to androgen receptor-antagonist therapy in prostate cancer. Proc Natl Acad Sci U S A. 2022;119(21):e2114324119.
13. Zhang Y, Qiu JG, Jia XY, Ke Y, Zhang MK, Stieg D, Liu WJ, Liu LZ, Wang L, Jiang BH. METTL3-mediated N6-methyladenosine modification and HDAC5/YY1 promote IFFO1 downregulation in tumor development and chemo-resistance. Cancer Lett. 2023;553:215971.
14. Zhang E, Han L, Yin D, He X, Hong L, Si X, Qiu M, Xu T, De W, Xu L, et al. H3K27 acetylation activated-long non-coding RNA CCAT1 affects cell proliferation and migration by regulating SPRY4 and HOXB13 expression in esophageal squamous cell carcinoma. Nucleic Acids Res. 2017;45(6):3086–101.
15. Zhang E, He X, Zhang C, Su J, Lu X, Si X, Chen J, Yin D, Han L, De W. A novel long noncoding RNA HOXC-AS3 mediates tumorigenesis of gastric cancer by binding to YBX1. Genome Biol. 2018;19(1):154.
16. Zhang C, Sun Q, Zhang X, Qin N, Pu Z, Gu Y, Yan C, Zhu M, Dai J, Wang C, et al. Gene amplification-driven RNA methyltransferase KIAA1429 promotes tumorigenesis by regulating BTG2 via m6A-YTHDF2-dependent in lung adenocarcinoma. Cancer Commun (Lond). 2022;42(7):609–26.
17. Dai J, Qu T, Yin D, Cui Y, Zhang C, Zhang E, Guo R. LncRNA LINC00969 promotes acquired gefitinib resistance by epigenetically suppressing of NLRP3 at transcriptional and posttranscriptional levels to inhibit pyroptosis in lung cancer. Cell Death Dis. 2023;14(5):312.
18. Zhu Q, Zhang C, Qu T, Lu X, He X, Li W, Yin D, Han L, Guo R, Zhang E. MNX1-AS1 promotes phase separation of IGF2BP1 to drive c-Myc-Mediated Cell-Cycle progression and proliferation in lung Cancer. Cancer Res. 2022;82(23):4340–58.
19. Kouzarides T. Chromatin modifications and their function. Cell. 2007;128(4):693–705.
20. Portela A, Esteller M. Epigenetic modifications and human disease. Nat Biotechnol. 2010;28(10):1057–68.
21. Zhang D, Tang Z, Huang H, Zhou G, Cui C, Weng Y, Liu W, Kim S, Lee S, Perez-Neut M, et al. Metabolic regulation of gene expression by histone lactylation. Nature. 2019;574(7779):575–80.
22. Wang Z, Wang Q, Chen C, Zhao X, Wang H, Xu L, Fu Y, Huang G, Li M, Xu J, et al. NNMT enriches for AQP5(+) cancer stem cells to drive malignant progression in early gastric cardia adenocarcinoma. Gut. 2023;73(1):63–77.
23. Wang Y, Zeng J, Wu W, Xie S, Yu H, Li G, Zhu T, Li F, Lu J, Wang GY, et al. Nicotinamide N-methyltransferase enhances chemoresistance in breast cancer through SIRT1 protein stabilization. Breast Cancer Res. 2019;21(1):64.
24. Eisenhauer EA, Therasse P, Bogaerts J, Schwartz LH, Sargent D, Ford R, Dancey J, Arbuck S, Gwyther S, Mooney M, et al. New response evaluation criteria in solid tumours: revised RECIST guideline (version 1.1). Eur J Cancer. 2009;45(2):228–47.
25. Pan Z, Wang K, Wang X, Jia Z, Yang Y, Duan Y, Huang L, Wu ZX, Zhang JY, Ding X. Cholesterol promotes EGFR-TKIs resistance in NSCLC by inducing EGFR/Src/Erk/SP1 signaling-mediated erralpha re-expression. Mol Cancer. 2022;21(1):77.
26. Di Biase S, Shim HS, Kim KH, Vinciguerra M, Rappa F, Wei M, Brandhorst S, Cappello F, Mirzaei H, Lee C, et al. Fasting regulates EGR1 and protects from glucose- and dexamethasone-dependent sensitization to chemotherapy. PLoS Biol. 2017;15(3):e2001951.
27. Liu Y, Kimpara S, Hoang NM, Daenthanasanmak A, Li Y, Lu L, Ngo VN, Bates PD, Song L, Gao X, et al. EGR1-mediated metabolic reprogramming to oxidative phosphorylation contributes to ibrutinib resistance in B-cell lymphoma. Blood. 2023;142(22):1879–94.
28. Yu J, Zhuang A, Gu X, Hua Y, Yang L, Ge S, Ruan J, Chai P, Jia R, Fan X. Nuclear PD-L1 promotes EGR1-mediated angiogenesis and accelerates tumorigenesis. Cell Discov. 2023;9(1):33.
29. Eckert MA, Coscia F, Chryplewicz A, Chang JW, Hernandez KM, Pan S, Tienda SM, Nahotko DA, Li G, Blazenovic I, et al. Proteomics reveals NNMT as a master metabolic regulator of cancer-associated fibroblasts. Nature. 2019;569(7758):723–8.
30. Lu S, Ke S, Wang C, Xu Y, Li Z, Song K, Bai M, Zhou M, Yu H, Yin B, et al. NNMT promotes the progression of intrahepatic cholangiocarcinoma by regulating aerobic Glycolysis via the EGFR-STAT3 axis. Oncogenesis. 2022;11(1):39.
31. Guo AS, Huang YQ, Ma XD, Lin RS. Mechanism of G9a inhibitor BIX–01294 acting on U251 glioma cells. Mol Med Rep. 2016;14(5):4613–21.
32. Wang JJ, Wang X, Xian YE, Chen ZQ, Sun YP, Fu YW, Wu ZK, Li PX, Zhou ES, Yang ZT. The JMJD3 histone demethylase inhibitor GSK-J1 ameliorates lipopolysaccharide-induced inflammation in a mastitis model. J Biol Chem. 2022;298(6):102017.
33. Chen Y, Yan H, Yan L, Wang X, Che X, Hou K, Yang Y, Li X, Li Y, Zhang Y, et al. Hypoxia-induced ALDH3A1 promotes the proliferation of non-small-cell lung cancer by regulating energy metabolism reprogramming. Cell Death Dis. 2023;14(9):617.
34. Parajuli B, Fishel ML, Hurley TD. Selective ALDH3A1 Inhibition by benzimidazole analogues increase Mafosfamide sensitivity in cancer cells. J Med Chem. 2014;57(2):449–61.
35. Wang X, Fan W, Li N, Ma Y, Yao M, Wang G, He S, Li W, Tan J, Lu Q, et al. YY1 lactylation in microglia promotes angiogenesis through transcription activation-mediated upregulation of FGF2. Genome Biol. 2023;24(1):87.
36. Yu J, Chai P, Xie M, Ge S, Ruan J, Fan X, Jia R. Histone lactylation drives oncogenesis by facilitating m(6)A reader protein YTHDF2 expression in ocular melanoma. Genome Biol. 2021;22(1):85.
37. Xiong J, He J, Zhu J, Pan J, Liao W, Ye H, Wang H, Song Y, Du Y, Cui B, et al. Lactylation-driven METTL3-mediated RNA m(6)A modification promotes immunosuppression of tumor-infiltrating myeloid cells. Mol Cell. 2022;82(9):1660–e16771610.
38. Chakraborty R, Ostriker AC, Xie Y, Dave JM, Gamez-Mendez A, Chatterjee P, Abu Y, Valentine J, Lezon-Geyda K, Greif DM, et al. Histone acetyltransferases p300 and CBP coordinate distinct chromatin remodeling programs in vascular smooth muscle plasticity. Circulation. 2022;145(23):1720–37.
39. Wu C, Liu Y, Liu W, Zou T, Lu S, Zhu C, He L, Chen J, Fang L, Zou L, et al. NNMT-DNMT1 Axis is essential for maintaining Cancer cell sensitivity to oxidative phosphorylation Inhibition. Adv Sci (Weinh). 2022;10(1):e2202642.
40. Cook PJ, Thomas R, Kingsley PJ, Shimizu F, Montrose DC, Marnett LJ, Tabar VS, Dannenberg AJ, Benezra R. Cox-2-derived PGE2 induces Id1-dependent radiation resistance and self-renewal in experimental glioblastoma. Neuro Oncol. 2016;18(10):1379–89.
41. Li W, Zhou C, Yu L, Hou Z, Liu H, Kong L, Xu Y, He J, Lan J, Ou Q, et al. Tumor-derived lactate promotes resistance to bevacizumab treatment by facilitating autophagy enhancer protein RUBCNL expression through histone H3 lysine 18 lactylation (H3K18la) in colorectal cancer. Autophagy. 2024;20(1):114–30.
42. Wang J, Liu X, Huang Y, Li P, Yang M, Zeng S, Chen D, Wang Q, Liu H, Luo K, et al. Targeting nicotinamide N-methyltransferase overcomes resistance to EGFR-TKI in non-small cell lung cancer cells. Cell Death Discov. 2022;8(1):170.
43. Yao H, Chen X, Wang T, Kashif M, Qiao X, Tuksammel E, Larsson LG, Okret S, Sayin VI, Qian H, et al. A MYC-controlled redox switch protects B lymphoma cells from EGR1-dependent apoptosis. Cell Rep. 2023;42(8):112961.
44. Bach DH, Kim D, Bae SY, Kim WK, Hong JY, Lee HJ, Rajasekaran N, Kwon S, Fan Y, Luu TT, et al. Targeting nicotinamide N-Methyltransferase and miR-449a in

EGFR-TKI-Resistant Non-Small-Cell lung Cancer cells. Mol Ther Nucleic Acids. 2018;11:455–67.
45. Zhang H, Zhang G, Xiao M, Cui S, Jin C, Yang J, Wu S, Lu X. Two-polarized roles of transcription factor FOSB in lung cancer progression and prognosis: dependent on p53 status. J Exp Clin Cancer Res. 2024;43(1):237.
46. Wang S, Cheng Z, Cui Y, Xu S, Luan Q, Jing S, Du B, Li X, Li Y. PTPRH promotes the progression of non-small cell lung cancer via Glycolysis mediated by the PI3K/AKT/mTOR signaling pathway. J Transl Med. 2023;21(1):819.
47. Liu Y, Qing B, Ke W, Wang M. MEK inhibitor Trametinib combined with PI3K/mTOR inhibitor BEZ-235 as an effective strategy against NSCLC through impairment of glucose metabolism. Cell Signal. 2024;124:111415.
48. Zong Z, Xie F, Wang S, Wu X, Zhang Z, Yang B, Zhou F. Alanyl-tRNA synthetase, AARS1, is a lactate sensor and lactyltransferase that lactylates p53 and contributes to tumorigenesis. Cell 2024.
49. Yu T, Liu Z, Tao Q, Xu X, Li X, Li Y, Chen M, Liu R, Chen D, Wu M, et al. Targeting tumor-intrinsic SLC16A3 to enhance anti-PD-1 efficacy via tumor immune microenvironment reprogramming. Cancer Lett. 2024;589:216824.
50. Ulanovskaya OA, Zuhl AM, Cravatt BF. NNMT promotes epigenetic remodeling in cancer by creating a metabolic methylation sink. Nat Chem Biol. 2013;9(5):300–6.
51. Xie X, Yu H, Wang Y, Zhou Y, Li G, Ruan Z, Li F, Wang X, Liu H, Zhang J. Nicotinamide N-methyltransferase enhances the capacity of tumorigenesis associated with the promotion of cell cycle progression in human colorectal cancer cells. Arch Biochem Biophys. 2014;564:52–66.
52. Duong HQ, You KS, Oh S, Kwak SJ, Seong YS. Silencing of NRF2 reduces the expression of ALDH1A1 and ALDH3A1 and sensitizes to 5-FU in pancreatic Cancer cells. Antioxid (Basel) 2017, 6(3).

Publisher's note